Growth of Well-Aligned γ-MnO_2 Monocrystalline Nanowires through a Coordination-Polymer-Precursor Route

Yujie Xiong,[a,b] Yi Xie,*[a,b] Zhengquan Li,[b] and Changzheng Wu[b]

Abstract: A new coordination-polymer-precursor route has been developed to synthesize nanowires under hydrothermal conditions. In the present work, well-aligned γ-MnO_2 nanowires, growing along the [002] axis, have successfully been prepared by selecting an appropriate coordination polymer $[\{Mn(SO_4)(4,4'\text{-bpy})(H_2O)_2\}_n]$ as precursor. In comparison with the experimental results from other coordination-polymer precursors, it is found that only $[\{Mn(SO_4)(4,4'\text{-bpy})(H_2O)_2\}_n]$ is appropriate for the formation of γ-MnO_2 crystal lattices during the process of oxidization. The IR absorption spectra of as-obtained precipitates at different reaction intervals minutely describe the reaction process, due to the different coordination abilities of ligands in the coordination polymer. More evidence about the mechanism will be further explored in the future study. Further observations show the ordered alignment of nanowires' tops and such well-aligned nanowires provide more possible applications in lithium batteries.

Keywords: coordination polymer · manganese · nanostructures · oxides · precursors

Introduction

Controlling the shape of nanostructures at the mesoscopic level is one of the most challenging issues presently faced by synthetic inorganic chemists.[1] Nanowires, which are one-dimensional objects, have been of special interest in the past few years, due to their unusual properties and potential applications.[2–9] Many methods have been used to prepare nanowires, such as electrochemistry,[2] template (mesoporous silica, carbon nanotubes, etc.),[3] emulsion or polymetric system,[4] arc discharge,[5] laser-assisted catalysis growth,[6] solution,[7] vapor transport,[8] organometallic and coordination chemistry methods.[9] The last method, which avoids complicated processes and special instruments, is more convenient to prepare nanowires. Most remarkably, this method attracts more attention to the relationship between structures of the target products and the raw materials, and is more appropriate for the phase control of products.

[a] Prof. Y. Xie, Dr. Y. Xiong
Structure Research Laboratory
University of Science and Technology of China
Hefei, Anhui 230026 (P. R. China)
Fax: (86) 551-3603987
E-mail: yxielab@ustc.edu.cn

[b] Prof. Y. Xie, Dr. Y. Xiong, Dr. Z. Li, Dr. C. Wu
Department of Chemistry
University of Science and Technology of China
Hefei, Anhui 230026 (P. R. China)

Once-dimensional systems, as the smallest dimension structures for efficient transport of electrons, can be applied to detect the theoretical operating limits of lithium batteries.[10] MnO_2 is widely used as a catalyst and as electrode material in Li/MnO_2 batteries;[11] this indicates the potential applications of MnO_2 nanowires. Recently, Li and co-workers have reported the hydrothermal preparation of α-MnO_2 nanowires and β-MnO_2 nanorods by oxidizing $MnSO_4$ in $KMnO_4$ and $K_2S_2O_8$, respectively.[12] Besides α- and β-phases, MnO_2 and the related manganese(IV) oxide are known to exist in a wide variety of structural forms, such as α-, β-, γ-, δ-type, ramsdellite, etc.[11] Among these phases, γ-MnO_2 is most commonly used as a cathode material in dry-cell batteries, and its electrical potential reduces more slowly than that of other forms during the process of discharge.[13] The unique characteristics of γ-MnO_2 will result in more important applications of γ-MnO_2 nanowires.

However, to our best knowledge, no report about the synthesis of γ-MnO_2 nanowires has been published to date, since the preparation of γ-MnO_2 needs greater amounts of energy.[13] In particluar, the most challenging problem of synthesizing γ-MnO_2 nanowires is how to control both the morphology and the phase of products. The phase control of products remains unsolved by the traditional methods for nanowires,[12] and the same problem also exists in preparing other metal oxide nanowires. The organometallic and coordination chemistry method should be dominant in the phase control of products. It is noteworthy that this method still cannot be extended to fabricate metal oxide nanowires up to now, although it has been greatly developed. Thus, we have

  0947-6539/03/0907-1645 $ 20.00+.50/0

tried to improve and apply the technique to the preparation of metal oxide nanowires. Certainly, selecting an appropriate precursor is crucial to control the phase and the morphology of metal oxide nanowires prepared by this method.

Herein, a new coordination-polymer-precursor route has been developed to synthesize nanowires under hydrothermal conditions. In the present work, well-aligned γ-MnO_2 nanowires, growing along [002] axis, have been successfully prepared by selecting an appropriate coordination polymer $[\{Mn(SO_4)(4,4'\text{-bpy})(H_2O)_2\}_n]$ as precursor.

Results and Discussion

Before we discuss our experimental results, we introduce our new strategy for the synthesis of metal oxide nanowires by a coordination-polymer-precursor route.

General route for metal oxide nanowires: The traditional organometallic and coordination chemistry methods can be simply classified into two sorts. One is to apply simple complexes or organometallic compounds[9] as precursors to produce metal or metal sulfide nanowires in liquid phase. The morphology control is mainly achieved by the oriented crystal growth of the desired materials, as a result of some structural characteristics in those precursors. It is a pity that the phase control of products is difficult to accomplish in this process, since no stable ordered and infinite structure exists in these precursors. The other is that coordination polymers can decompose to films of the desired materials by a CVD route,[14] in which the phase of products is more easily controlled. However, the formation of one-dimensional nanostructures seems impossible at such high temperatures without vapor transport process.

From the above analyses, a new coordination-polymer-precursor route under hydrothermal conditions has been developed for the synthesis of metal oxide nanowires. Previous researches in coordination chemistry indicate that many coordination polymers have stable, ordered structures. In particular, the metal cations in some coordination polymers bridged by rigid ligands (e.g., 4,4′-bpy) are not only ordered, but also have different coordination modes. From the appropriate selection of a coordination polymer as a precursor, it is possible to make the polymer dissociate and form new metal–oxygen bonds under alkaline hydrothermal conditions, forming the desired metal oxide. In the process of the oxidization reaction, the different coordination abilities of the ligands in the polymer will probably lead to a faster oxidization along some direction, thus resulting in an oriented growth of metal oxide nanowires. Hence, we have designed a hydrothermal route to synthesize metal oxide nanowires through an alkaline replacement reaction on coordination-polymer precursors.

Synthesis route: Based on the above strategy, γ-MnO_2 nanowires were prepared as follows. The coordination polymer $[\{Mn(SO_4)(4,4'\text{-bpy})(H_2O)_2\}_n]$ was first prepared in a mixed solvent of CH_3OH and H_2O at room temperature.[15] The as-obtained coordination-polymer crystals were then transformed into γ-MnO_2 nanowires in air by boiling a soltion of them in NaOH. The chemical reaction can be given as Equation (1):

$$[\{Mn(SO_4)(4,4'\text{-bpy})(H_2O)_2\}_n] + n/2\,O_2 + 2n\,OH^- \rightarrow n\gamma\text{-}MnO_2 + 3n\,H_2O + n\,SO_4^{2-} + n\,4,4'\text{-bpy} \quad (1)$$

The replacement process of ligands by oxygen anions is shown in Scheme 1.The proportion of nanowires in the product is above 90%, and their yield is about 40% based on the original reagents.

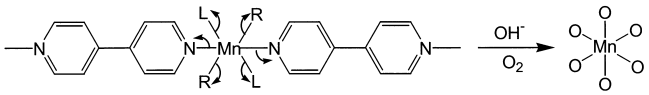

Scheme 1. The reaction process from $[\{Mn(SO_4)(4,4'\text{-bpy})(H_2O)_2\}_n]$ to the γ-MnO_2 crystall lattice.

Phase and purity of the obtained product

XRD pattern: The crystal data of coordination-polymer precursor were investigated by measurements on an Enraf-Nonius CAD-4 diffractometer; these data agree well with the reported data for $[\{Mn(SO_4)(4,4'\text{-bpy})(H_2O)_2\}_n]$.[15] Therefore, it is not necessary to provide the detailed crystal data here. The phase and purity of as-obtained product was determined by the X-ray diffraction (XRD) pattern, shown in Figure 1.

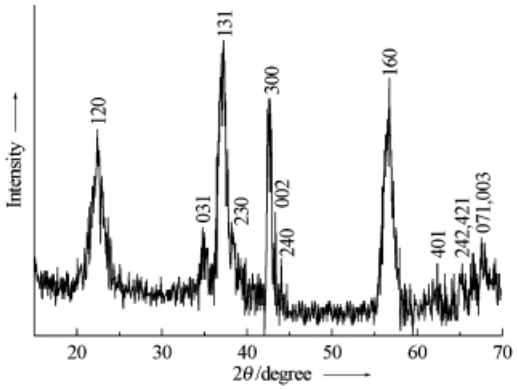

Figure 1. XRD pattern of the as-obtained γ-MnO_2 nanowires.

All the reflection peaks can be indexed to pure orthorhombic γ-MnO_2 (JCPDS card 14-644, a = 6.36 Å, b = 10.15 Å, c = 4.09 Å). The intensity of (002) peak was slightly improved in the obtained XRD pattern. No characteristic peaks were observed for other impurities such as α-, β-MnO_2, $Mn(OH)_2$, and $Mn(OH)_4$.

XPS spectra: Important information about the surface molecular and electronic structure of the as-obtained product was provided by X-ray photoelectron spectra (XPS). The binding energies obtained in the XPS analysis were corrected for specimen charging by referencing C 1s to 284.60 eV. The Mn 2p core level spectrum (Figure 2A) illustrates that the observed values of the binding energies for Mn $2p_{3/2}$ and Mn $2p_{1/2}$ (642.1 eV and 653.6 eV, respectively) are in agree-

0947-6539/03/0907-1646 $ 20.00+.50/0 *Chem. Eur. J.* **2003**, *9*, No. 7

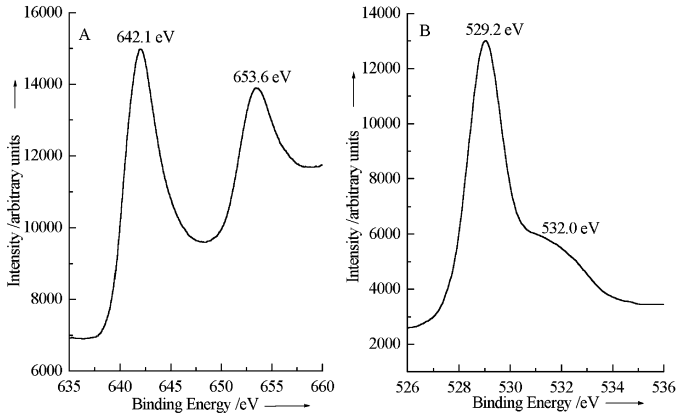

Figure 2. A) Mn 2p core level spectrum of γ-MnO_2 nanowires. B) O 1s core level spectrum of γ-MnO_2 nanowires.

ment with the literature values of bulk for Mn^{2+}.[16] The O 1s binding energy (Figure 2B; 529.2 eV) indicates that the oxygen atoms exist as O^{2-} species in the compounds.[16] The weak shoulder at $\sim$532.0 eV in the spectra of γ-MnO_2 nanowires is ascribed to oxygen from absorbed gaseous molecules. All these results indicate that the sample is MnO_2, and the XPS survey spectra show that no obvious impurities detected in the samples; this indicates that the level of impurities present is lower than the resolution limit of XPS (1 at.%).

Raman spectra: Raman spectroscopy (Figure 3), a powerful experimental technique for the identification and characterization of the local Mn environment, further confirms our

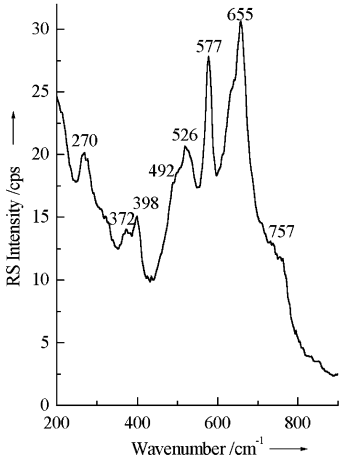

Figure 3. Raman spectrum of γ-MnO_2 nanowires.

product as γ-MnO_2. The structural arrangement of γ-MnO_2 is usually explained by a random intergrowth of pyrolusite layers in a ramsdellite (R-MnO_2) matrix. The Raman data for manganese dioxides with the γ-type structure can be treated by a local environment model, which allows us to consider the relationship between the band wavenumber and the pyrolusite intergrowth that corresponds to the structural DeWolff defects. The peaks in the wavenumber range of 500–700 cm^{-1} are considered as the characteristic features of γ-MnO_2. A close examination of this spectral region shows that for the three main bands of R-MnO_2 (denoted as ν_1, ν_2, and ν_3), a wavenumber shift of the bands ν_1 and ν_3 occurs toward those of the β-MnO_2 phase (at higher wavenumber), whereas ν_2 remains at almost the same position. This indicates that the amount of pyrolusite defects increases in the ramsdellite network. The pyrolusite-like peak located at 630 cm^{-1} appears as a shoulder in the γ-MnO_2 phase and the band at 654 cm^{-1} is located between ν_1 of R-MnO_2 (630 cm^{-1}) and ν_1 of β-MnO_2 (665 cm^{-1}). All these features confirm that our product is γ-MnO_2.[17]

The morphology and growth direction of the obtained product: The panoramic morphologies of obtained product were examined by the field emission scanning electron microscopy (FE-SEM), in which the solid sample was mounted on a copper mesh without any dispersion treatment. The results indicate that the product consists of nanowires with diameters of 20–40 nm on average and lengths ranging from 3–6 μm. The proportion of nanowires in the product is above 90% and their yield is about 40% based on the original reagents. The FE-SEM image of the center of sample (Figure 4A) shows the uniform nanowires, while that of the sample fringe (Figure 4B) shows that the tops of nanowires almost align along one direction. This ordered alignment of γ-MnO_2 nanowires may lead to more applications in lithium batteries.

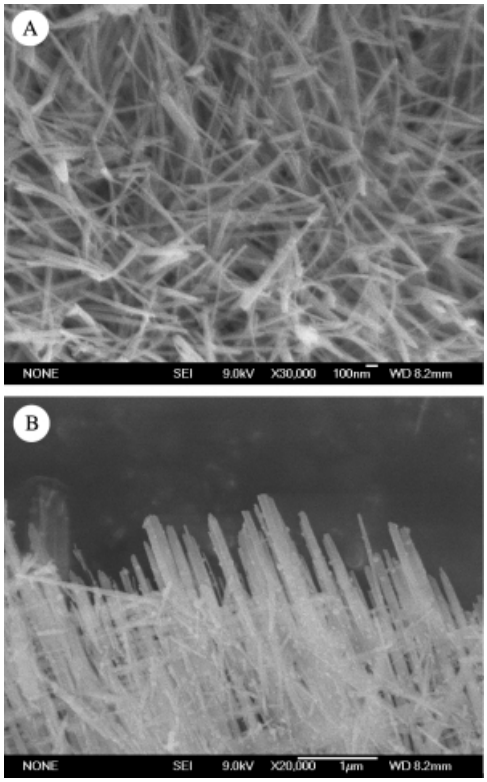

Figure 4. FE-SEM image of the as-obtained γ-MnO_2 nanowires.

More details about the structure of nanowires were investigated by the electronic diffraction (ED) patterns and high-resolution transmission electron microscopy (HRTEM). The HRTEM images (Figure 5A and C) of the nanowires shows that the obtained wires are structurally uniform and

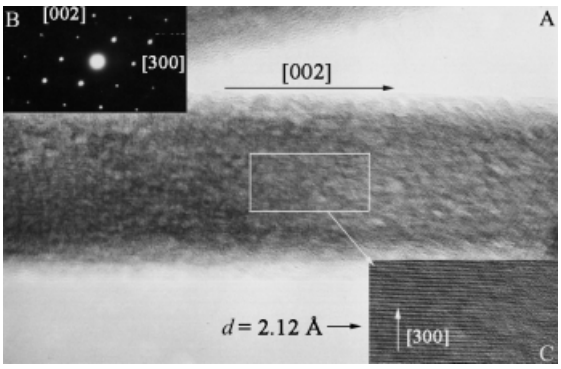

Figure 5. A) HRTEM image of the as-obtained γ-MnO_2 nanowires. B) ED pattern of a γ-MnO_2 nanowire. C) Enlargement of the HRTEM image.

monocrystalline. Meanwhile, the ED pattern (Figure 5B) further confirms that the obtained product is monocrystalline, growing along [002] direction.

Possible mechanism of forming γ-MnO_2 nanowires: The same reaction process has been carried out with other coordination polymers (e.g., $[\{Mn(N_3)_2(4,4'\text{-bpy})\}_n]$)[15] as precursors, and no γ-MnO_2 nanowires could be obtained. If the two experimental steps were simplified to one (i.e., before the coordination polymer crystals separated out from the matrix solution, NaOH was directly added into the solution and then hydrothermal treatment applied), γ-MnO_2 nanowires could not be obtained either. This implies that the crystal structure of the coordination polymer is crucial to the formation of γ-MnO_2 nanowires. However, considering the reaction process, the structure of polymer should be immediately irrelevant to the formation of oxide nanowires, if the coordination polymer was fully dissociated in the boiling NaOH before forming new Mn–O bonds of γ-MnO_2.

To investigate the dissociation process of the Mn-ligand moieties, the IR absorption spectrum of the precursor was measured (Figure 6A). In the far-IR region, the absorption peaks at 292, 348, and 403 cm^{-1} are the Mn–N (in bpy),[18] the Mn–O (in H_2O),[19] and the Mn–O (in SO_4^{2-}) stretching vibrations,[20] respectively. By comparison, the obtained precipitates after reaction times of 1.5, 2.5, and 4.5 h were also determined by IR spectra. It was found that the absorption peaks of the Mn–O (in H_2O), Mn–O (in SO_4^{2-}), and Mn–N (in bpy) stretching vibration gradually disappeared in turn. On the other hand, the absorption peaks at 418–430 cm^{-1}, which were assigned to the Mn–O stretching vibration of γ-MnO_2,[20,21] appeared and their intensity increased with increasing reaction times. This means that the Mn atoms wwere dissociated from the water SO_4^{2-}, and bpy ligands in turn, while the new Mn–O bonds of γ-MnO_2 formed; this agrees with the fact that coordination polymers which contain 4,4′-bpy ligands are usually stable. These characterization results reveal that the dissociation of the coordination polymer and the formation of γ-MnO_2 occurred at the same time, and the water ligands were dissociated first. Thus, the structural correlation between the polymer and the oxide is probably relevant.

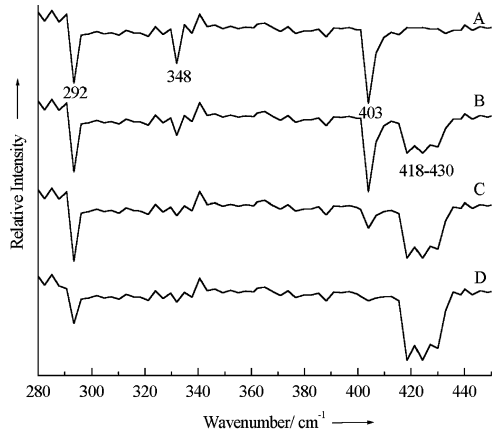

Figure 6. A) IR spectrum of coordination-polmer precursor. B)–D) IR spectra of the as-obtained precipitates after reaction for 1.5, 2.5, and 4.5 h, respectively.

In the following paragraphs, we try to investigate the effect of the coordination polymer on the growth of γ-MnO_2 nanowires with respect to the structural relationship. In Figures 7, 8, and 9, by taking the relative positions of the metal cations into consideration, the structures of coordination polymer and γ-MnO_2 can be simplified into various frameworks of metal cations that are supported by the rigid ligands and oxygen anions, respectively. The thin lines only represent the distance between the Mn cations.

γ-MnO_2 is considered to be a disordered intergrowth of the β-MnO_2 and ramsdellite structures, consisting of a random arrangement of single and double chains of MnO_6 octahedra (Figure 7).[22] From the planform depiction of the γ-MnO_2

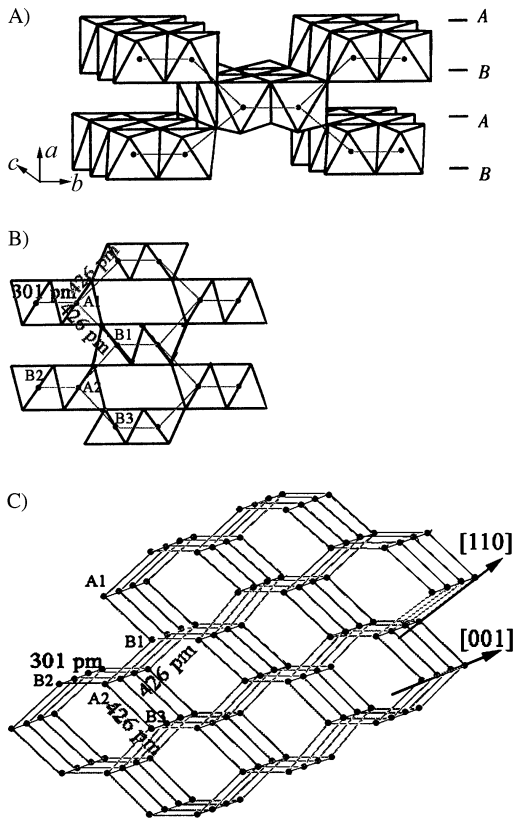

Figure 7. A) The structure of γ-MnO_2. B) The planform perpendicular to the chains. C) The framework of the Mn cations in the γ-MnO_2 crystal latticew. The thin lines represent the distance between the Mn cations.

0947-6539/03/0907-1648 $ 20.00+.50/0 *Chem. Eur. J.* **2003**, *9*, No. 7

structure (Figure 7B), it is found that each Mn cation is connected to three adjacent cations through oxygen anions to build up distorted Mn hexagonal units in layers, which are composed of Mn cation frameworks shown in Figure 7C. The layers (parallel to *ab* plane) are also connected by sharing oxygen anions.

It is found that the coordination polymer [{Mn(SO_4)(4,4′-bpy)(H_2O)$_2$}$_n$] has an infinite, three-dimensional layer structure (Figure 8A),[15] in which each layer is formed in the *ac* plane by Mn centers connected through bridging bpy ligands to generate parallel -Mn-bpy-Mn-bpy chains; between adjacent layers the -Mn-bpy-Mn-bpy chains have an angle of 45°. The -Mn-bpy-Mn-bpy chains in different layers are connected by zigzag -Mn-SO_4^{2-}-Mn-SO_4^{2-} chains, leading to a three-dimensional polymer framework. Comparing the distances Mn(A2)–Mn(A1) and Mn(A2)–Mn(A3) with Mn(A2)–Mn(B1), Mn(A2)–Mn(B2), and Mn(A2)–Mn(B3) (Figure 8), one can see that the first two distances are much larger than the last three. When the precursor of coordination polymer is gradually dissociated in the boiling NaOH, the nearest Mn cations have more chance to combine with each other and form stable manganese(IV) oxide through the bridging of oxygen anions. Thus, Mn(A2) will most probably connect with the nearest Mn(B1), Mn(B2), and Mn(B3) cations through oxygen anion bridges. These nearest neighbor Mn cations can also be described as distorted hexagonal units in layers (Figure 8B). It is found that the structural features of these Mn cations are similar to those in γ-MnO_2 crystal lattices. Certainly, other possible factors exist that may affect reaction process; however, the above structural similarity seems to be the most probable.

More careful studies on the structure of [{Mn(SO_4)(4,4′-bpy)(H_2O)$_2$}$_n$] show that the Mn distorted hexagonal units arrange in layers. These layers deviate from the *ac* plane and each of them is separated by oxygen donors from two water ligands. This characteristic can be clearly shown in the CDEF section of the structure of coordination-polymer precursor (Figure 9A). Comparing this section with the $(1\bar{1}0)$ section of γ-MnO_2 crystal lattices (Figure 9B), we find that the two sections are similar in structure and that the coordination direction of Mn–water bonds in coordination-polymer precursor seems to correspond to the [001] axis of γ-MnO_2 crystal lattices. Mn–water bonds perpendicular to the layers were the first to dissociate in boiling NaOH, probably leading to the oriented growth of γ-MnO_2 crystal lattices to nanowires along [002] axis. The ordered alignment of γ-MnO_2 nanowires might also result from the -Mn-bpy-Mn-bpy- connection, the last one to be dissociated.

All the above is the possible mechanism proposed on the base of the present experimental results. More information about the mechanism will be further explored in a future study.

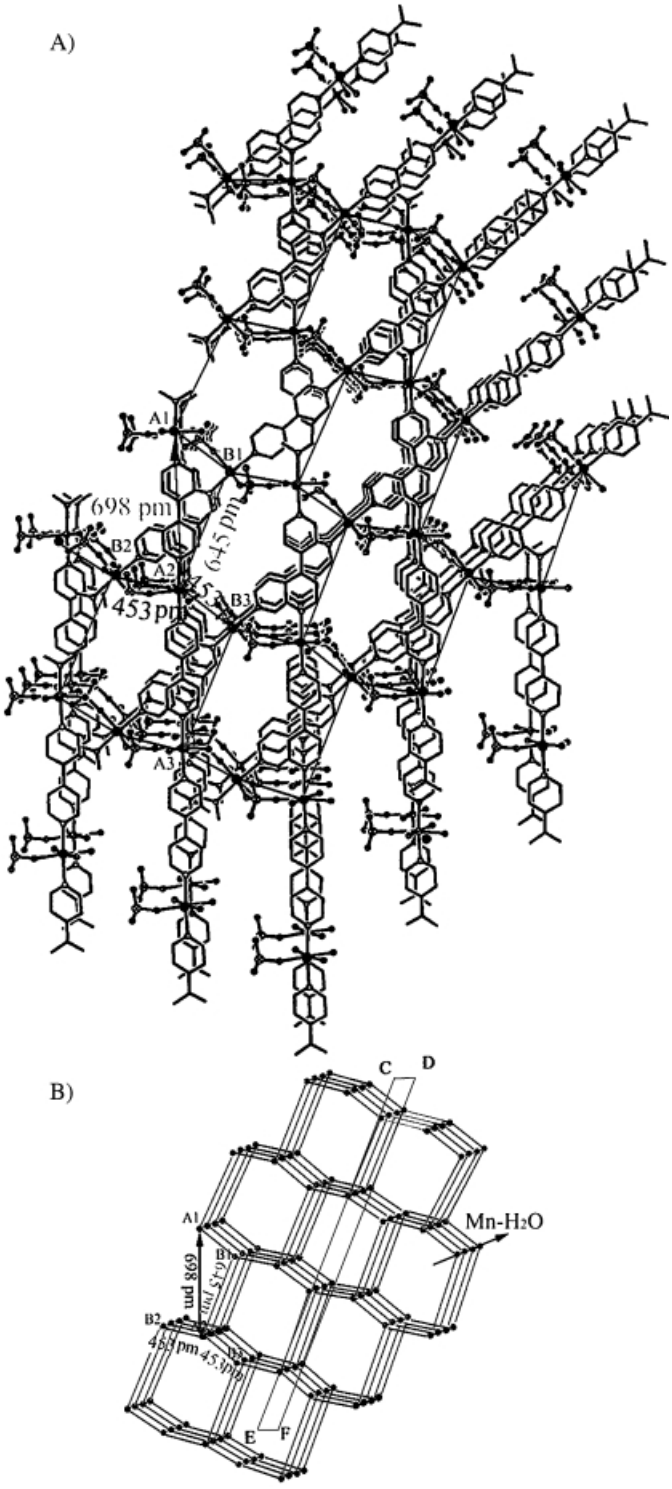

Figure 8. A) The structure of the coordination polymer [{Mn(SO_4)(4,4′-bpy)(H_2O)$_2$}$_n$]. B) The nearest neighbor Mn cations that have the best opportunity to combine with each other to from stable manganese(IV) oxide, when dissociation in boiling NaOH occurs. The dashed lines correspond to the two directions of -Mn-bpy-Mn-bpy- cahins. The thin lines represent the distance between the Mn cations.

Conclusion

In summary, a new coordination-polymer-precursor route has been developed to synthesize nanowires under hydrothermal conditions. In this work, well-aligned γ-MnO_2 nanowires, growing along the [002] axis, have been successfully prepared by selecting an appropriate coordination polymer, [{Mn(SO_4)(4,4′-bpy)(H_2O)$_2$}$_n$], as the precursor. In compar-

  0947-6539/03/0907-1649 $ 20.00+.50/0

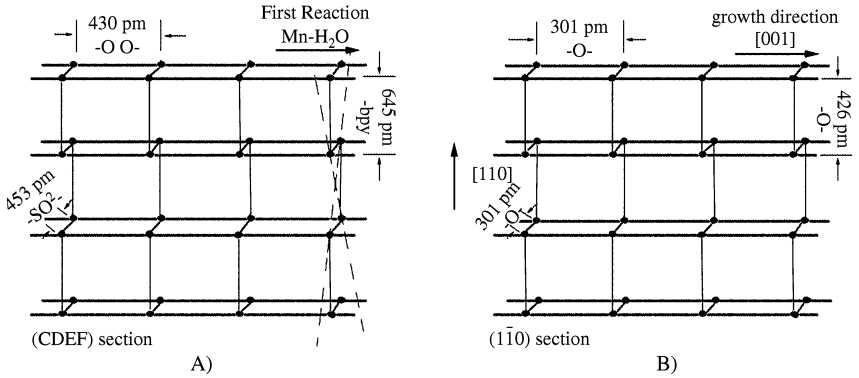

Figure 9. A) The CDEF section (indicated in Figure 8) of the structure of the coordination-polymer precursor. The dashed lines correspond to the two directions of -Mn-bpy-Mn-bpy- cahins. B) The (1$\bar{1}$0) section of the γ-MnO_2 lattice. The solid lines represent the distance between the Mn cations.

ison with the experimental results from other coordination-polymer precursors, it is found that only [{$Mn(SO_4)$(4,4′-bpy)$(H_2O)_2$}$_n$] is appropriate for the formation of γ-MnO_2 crystal lattices during the process of oxidization. The IR absorption spectra of the obtained precipitates at different reaction intervals minutely describe the reaction process and show the different coordination abilities of ligands in the coordination polymer. Further observations show the ordered alignment of nanowires' tops, and such well-aligned nanowires may provide more possible applications in lithium batteries. The simple process, excellent reproducibility, clean reactions, high yield, and fine quality of products in this work make it possible to scale up to industrial production. This strategy is expected to extend to the synthesis of other metals or compounds nanowires.

Experimental Section

Preparation of [{$Mn(SO_4)$(4,4′-bpy)$(H_2O)_2$}$_n$]: In a typical experiment, similar to that given in the literature,[15] 4,4′-bpy (0.078 g, 0.5 mmol) was dissolved in CH_3OH (3 mL). $MnSO_4 \cdot H_2O$ (0.0845 g, 0.5 mmol) in H_2O (5 mL) was added dropwise at room temperature. A clear solution was obtained, and some colorless crystals were then produced after several days. The as-obtained crystals were collected for the second reaction process. The crystal data of coordination-polymer precursor were investigated on an Enraf-Nonius CAD-4 diffractometer and are in agreement with the reported data for [{$Mn(SO_4)$(4,4′-bpy)$(H_2O)_2$}$_n$].[15]

Preparation of γ-MnO_2 nanowires: The above as-obtained [{$Mn(SO_4)$(4,4′-bpy)$(H_2O)_2$}$_n$] (0.2 g) and NaOH (0.04 g, 1 mmol) were loaded into a 100 mL Teflon-lined autoclave, which was then filled with distilled water up to 80% of the total volume. The autoclave was sealed, warmed up at a speed of 1 °C min^{-1}, maintained at 120 °C for 12 h, and was then cooled to room temperature naturally. The precipitate was filtered off, washed with absolute ethanol and distilled water for several times, and then dried in vacuum at 60 °C for 4 h. The proportion of nanowires in the product was above 90% and their yield was about 40% based on the original reagents.

Characterization: The X-ray diffraction (XRD) patterns were determined on a Japan Rigaku D/max γA X-ray diffractometer equipped with graphite monochromatized high-intensity $Cu_{K\alpha}$ radiation ($\lambda = 1.54178$ Å). The X-ray photoelectron spectra (XPS) were collected on an ESCALab MKII X-ray photoelectron spectrometer, with non-monochromatized $Mg_{K\alpha}$ X-ray as the excitation source. The Raman spectra were recorded at room temperature on a LABRAM-HR Confocal Laser MicroRaman spectrometer. IR absorption spectra were performed with a Nicolet FT-IR-170SX spectrometer in the range of 250–450 cm^{-1} at room temperature, with the sample in a KBr disk. The field emission scanning electron microscopy (FE-SEM) images were taken on a JEOL JSM-6700F SEM. The electronic diffraction (ED) patterns and high-resolution transmission electron microscopy (HRTEM) images were carried out on a JEOL-2010 TEM at an acceleration voltage of 200 KV.

Acknowledgement

This work was supported by the Chinese National Natural Science Foundation and the foundation for the Author of National Excellent Doctoral Dissertation of P. R. China (Project No. 199923). The authors thank Prof. Shuyuan Zhang and Mr. Ke Jiang for technical assistance in HRTEM and FE-SEM experiments, respectively.

[1] A. P. Alivisatos, *Science* **1996**, *271*, 933.
[2] a) Y. Zhou, S. H. Yu, X. P. Cui, C. Y. Wang, Z. Y. Chen, *Chem. Mater.* **1999**, *11*, 545; b) J. J. Zhu, S. W. Liu, O. Palchik, Y. Koltypin, A. Gedanken, *Langmuir* **2000**, *16*, 6396; c) D. Xu, Y. Xu, D. Chen, G. Guo, L. Gui, Y. Tang, *Adv. Mater.* **2000**, *12*, 520.
[3] a) C. R. Martin, *Science* **1994**, *266*, 1961; b) M. H. Huang, A. Choudrey, P. D. Yang, *Chem. Commun.* **2000**, 1063; c) C. Tang, S. Fan, M. Lamy de la Chapelle, H. Dang, P. Li, *Adv. Mater.* **2000**, *12*, 1346.
[4] a) S. Bhattacharrya, S. K. Saha, D. Chakravorty, *Appl. Phys. Lett.* **2000**, *76*, 3896; b) S. W. Liu, J. Yue, A. Gedanken, *Adv. Mater.* **2001**, *13*, 656; c) S. Bhattacharrya, S. K. Saha, D. Chakravorty, *Appl. Phys. Lett.* **2000**, *77*, 3770; d) N. R. Jana, L. Gearheart, C. L. Murphy, *Chem. Commun.* **2001**, 617.
[5] a) S. Iijima, *Nature* **1991**, *354*, 56; b) T. Seeger, P. Kohler-Redlich, M. Ruhle, *Adv. Mater.* **2000**, *12*, 279.
[6] a) A. M. Morales, C. M. Lieber, *Science* **1998**, *279*, 208; b) M. S. Gudiken, C. M. Lieber, *J. Am. Chem. Soc.* **2000**, *122*, 8801.
[7] a) T. J. Trentler, K. M. Hickman, S. C. Goel, A. M. Viano, P. C. Gibbons, W. E. Buhro, *Science* **1995**, *270*, 1791; b) B. Gates, Y. Yin, Y. Xia, *J. Am. Chem. Soc.* **2000**, *122*, 12582.
[8] Y. Wu, P. Yang, *Chem. Mater.* **2000**, *12*, 605.
[9] a) K. Soulantica, A. Maisonnat, F. Senocq, M. C. Fromen, M. J. Casanove, B. Chaudret, *Angew. Chem.* **2001**, *113*, 3071; *Angew. Chem. Int. Ed.* **2001**, *40*, 2983; b) P. Yan, Y. Xie, Y. Qian, X. Liu, *Chem. Commun.* **1999**, 1293.
[10] a) B. Ammundsen, J. Paulsen, *Adv. Mater.* **2001**, *13*, 943; b) H. Itoh, S. Nagano, T. Urata, E. Kikuchi, *Appl. Catal.* **1991**, *77*, 37.
[11] a) M. H. Huang, S. Mao, H. Feick, H. Yan, Y, Wu, H. Kind, E. Weber, R. Russo, P. Yang, *Science* **2001**, *292*, 1897; b) J. T. Hu, T. W. Odom, C. M. Lieber, *Acc. Chem. Res.* **1999**, *32*, 435.
[12] a) X. Wang, Y. Li, *J. Am. Chem. Soc.* **2002**, *124*, 2880; b) X. Wang, Y. Li, *Chem. Commun.* **2002**, 764.
[13] a) A. J. Kramer, J. J. M. Janssen, J. A. A. J. Perenboom, *IEEE Trans. Magn.* **1990**, *26*, 1858; b) J. M. Tarascon, *Mater. Tech.* **1993**, *8*, 39.
[14] a) B. J. Bae, J. E. Park, B. Kim, J. T. Park, *J. Organomet. Chem.* **2000**, *616*, 128; b) L. Grocholl, J. Wang, E. G. Gillan, *Chem. Mater.* **2001**, *13*, 4290.
[15] H. Hou, Y. Wei, Y. Fan, C. Du, Y. Zhu, Y. Song, Y. Niu, X. Xin, *Inorg. Chim. Acta* **2001**, *319*, 212.
[16] C. D. Wanger, W. M. Riggs, L. E. Davis, J. F. Moulder, G. E. Muilenberg, *Handbook of X-ray Photoelectron Spectroscopy*, Perkin – Elmer, Eden Prairie, **1978**.
[17] C. Julien, M. Massot, S. Rangan, M. Lemal, D. Guyomard, *J. Raman Spectrosc.* **2002**, *33*, 223.
[18] Z. J. Li, C. R. Liu, G. W. Lian, *Chin. Chem. Lett.* **1994**, *15*, 4.
[19] D. M. Adams, P. J. Lock, *J. Chem. Soc. A* **1971**, 2801.

  0947-6539/03/0907-1650 $ 20.00+.50/0

[20] N. Kazou, *Infrared and Raman Spectra of Inorganic and Coordination Compounds*, Wiley, New York, **1977**.
[21] Q. Feng, H. Kanoh, Y. Miyai, K. Ooi, *Chem. Mater.* **1995**, *7*, 1226.
[22] a) J. C. Hunter, *J. Solid State Chem.* **1981**, *39*, 142; b) *Manganese Dioxide Symp.* **1970**, *1*, whole volume; c) Y. Qian, *Introduction to Crystallography*, University of Science and Technology Press, Hefei, **1999** (in Chinese).

Received: September 20, 2002
Revised: January 20, 2003 [F4440]

  0947-6539/03/0907-1651 $ 20.00+.50/0